Double-β Decay

OMITTED FROM SUMMARY TABLE

NEUTRINOLESS DOUBLE-β DECAY

Revised August 2005 by P. Vogel (Caltech) and A. Piepke (University of Alabama).

Neutrinoless double-beta ($0\nu\beta\beta$) decay would signal violation of the total lepton number conservation. The process can be mediated by an exchange of a light Majorana neutrino, or by an exchange of other particles. However, the existence of $0\nu\beta\beta$-decay requires Majorana neutrino mass, no matter what the actual mechanism is. As long as only a limit on the lifetime is available, limits on the effective Majorana neutrino mass, and on the lepton-number violating right-handed current or other possible mechanisms mediating $0\nu\beta\beta$ decay can be obtained, independently on the actual mechanism. These limits are listed in the next three tables, together with a claimed $0\nu\beta\beta$-decay signal reported by part of the Heidelberg-Moscow collaboration. There, a 4σ excess of counts at the decay energy is used for a determination of the Majorana neutrino mass. This signal has not yet been independently confirmed. In the following we *assume* that the exchange of light Majorana neutrinos ($m_i \leq \mathcal{O}(10\ \mathrm{MeV})$) contributes dominantly to the decay rate.

Besides a dependence on the phase space ($G^{0\nu}$) and the nuclear matrix element ($M^{0\nu}$), the observable $0\nu\beta\beta$-decay rate is proportional to the square of the effective Majorana mass $\langle m_{\beta\beta}\rangle$, $(T^{0\nu}_{1/2})^{-1} = G^{0\nu} \cdot |M^{0\nu}|^2 \cdot \langle m_{\beta\beta}\rangle^2$, with $\langle m_{\beta\beta}\rangle^2 = |\sum_i U^2_{ei} m_i|^2$. The sum contains, in general, complex CP phases in U^2_{ei}, *i.e.*, cancellations may occur. For three neutrino flavors, there are three physical phases for Majorana neutrinos and one for Dirac neutrinos. The two additional Majorana phases affect only

processes to which lepton-number changing amplitudes contribute. Given the general 3×3 mixing matrix for Majorana neutrinos, one can construct other analogous lepton number violating quantities, $\langle m_{\ell\ell'} \rangle = \sum_i U_{\ell i} U_{\ell' i} m_i$. However, these are currently much less constrained than $\langle m_{\beta\beta} \rangle$.

Nuclear structure calculations are needed to deduce $\langle m_{\beta\beta} \rangle$ from the decay rate. While $G^{0\nu}$ can be calculated reliably, the computation of $M^{0\nu}$ is subject to uncertainty. Indiscriminate averaging over all published matrix element values would result, for any given nuclide, in a factor of $\sim$3 uncertainty in the derived $\langle m_{\beta\beta} \rangle$ values. More recent evaluations, insisting that the known $2\nu\beta\beta$ rate is correctly reproduced, result in a considerable reduction in the spread of the $M^{0\nu}$ values. *E.g.* in [1], the spread appears to be as low as $\pm 30\%$. The particle physics quantities to be determined are thus nuclear model-dependent, so the half-life measurements are listed first. Where possible, we reference the nuclear matrix elements used in the subsequent analysis. Since rates for the more conventional $2\nu\beta\beta$ decay serve to calibrate the nuclear theory, results for this process are also given.

Oscillation experiments utilizing atmospheric-, accelerator-, solar-, and reactor-produced neutrinos and anti-neutrinos yield strong evidence that at least some neutrinos are massive. However, these findings shed no light on the 3,1 mass hierarchy, the absolute neutrino mass values, or the properties of neutrinos under CPT-conjugation (Dirac or Majorana).

If the, thus far unconfirmed, LSND evidence is set aside all oscillation experiments can be consistently described using three interacting neutrino species with two mass splittings and three mixing angles. Full three flavor analyses such as *e.g.* [2] yield: $\Delta m^2_{atm} \sim (2.4^{+0.5}_{-0.6}) \times 10^{-3}$ eV^2 and $\sin^2 \theta_{atm} = 0.44^{+0.18}_{-0.10}$ for the parameters observed in atmospheric and accelerator

experiments. Oscillations of solar ν_e and reactor $\bar{\nu}_e$ lead to $\Delta m^2_{\odot} = (7.92 \pm 0.71) \times 10^{-5}$ eV^2 and $\sin^2\theta_{\odot} = 0.314^{+0.057}_{-0.047}$ (all errors at 95% CL). The investigation of reactor $\bar{\nu}_e$ at $\sim$1 km baseline, combined with solar neutrino and long baseline reactor experiments, indicates that electron type neutrinos couple only weakly to the third mass eigenstate with $\sin^2\theta_{13} < 0.03$. The so called 'LSND evidence' for oscillations at short baseline requires $\Delta m^2 \sim 0.2 - 2$ eV^2 and small mixing. If confirmed by the ongoing MiniBooNE experiment, this phenomenon would require the addition of at least one more non-interacting neutrino species.

Based on the 3-neutrino analysis: $\langle m_{\beta\beta}\rangle^2 \approx |\cos^2\theta_{\odot}\ m_1 + e^{i\Delta\alpha_{21}} sin^2\theta_{\odot}\ m_2 + e^{i\Delta\alpha_{31}} \sin^2\theta_{13}\ m_3|^2$, with $\Delta\alpha_{21}, \Delta\alpha_{31}$ denoting the physically relevant Majorana CP-phase differences (possible Dirac phase δ is absorbed in these $\Delta\alpha$). Given the present knowledge of the neutrino oscillation parameters one can derive the relation between the effective Majorana mass and the mass of the lightest neutrino, as illustrated in the left panel of Fig. 1. The three mass hierarchies allowed by the oscillation data: normal ($m_1 < m_2 < m_3$), inverted ($m_3 < m_1 < m_2$), and degenerate ($m_1 \approx m_2 \approx m_3$), result in different projections. The width of the innermost hatched bands reflects the uncertainty introduced by the unknown Majorana phases. If the experimental errors of the oscillation parameters are taken into account, then the allowed areas are widened as shown by the outer bands of Fig. 1. Because of the overlap of the different mass scenarios, a measurement of $\langle m_{\beta\beta}\rangle$ in the degenerate or inversely hierarchical ranges would not determine the hierarchy. The middle panel of Fig. 1 depicts the relation of $\langle m_{\beta\beta}\rangle$ with the summed neutrino mass $M = m_1 + m_2 + m_3$, constrained by observational cosmology. The oscillation data

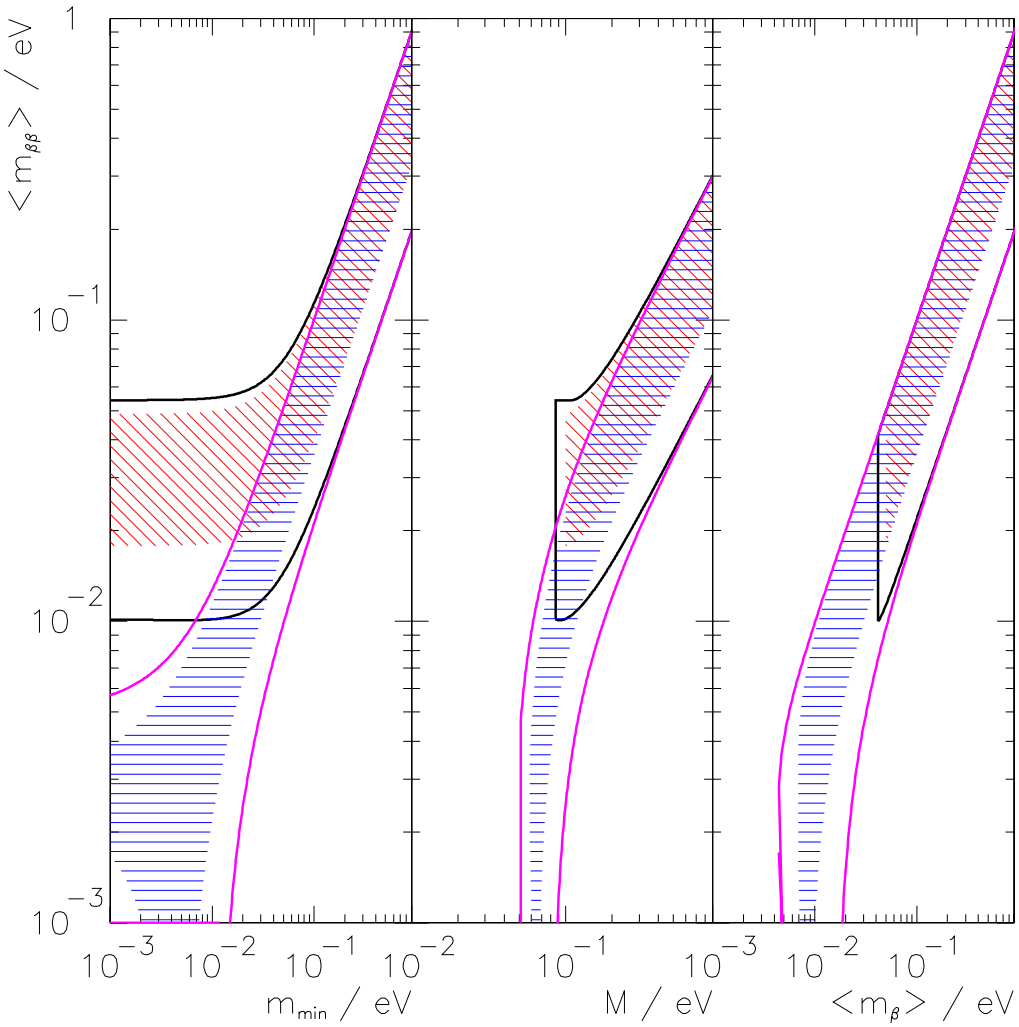

Figure 1: The left panel shows the dependence of $\langle m_{\beta\beta}\rangle$ on the absolute mass of the lightest neutrino m_{min}. The middle panel shows $\langle m_{\beta\beta}\rangle$ as a function of the summed neutrino mass M, while the right panel depicts $\langle m_{\beta\beta}\rangle$ as a function of the mass $\langle m_{\beta}\rangle$. In all panels the width of the hatched areas is due to the unknown Majorana phases and thus irreducible. The allowed areas given by the solid lines are obtained by taking into account the errors of the oscillation parameters. The two sets of solid lines correspond to the normal and inverted hierarchies. These sets merge into each other for $\langle m_{\beta\beta}\rangle \geq 0.1$ eV, which corresponds to the degenerate mass pattern. See full-color version on color pages at end of book.

thus allow to test whether observed values of $\langle m_{\beta\beta}\rangle$ and M are consistent within the 3 neutrino framework. The right hand panel of Fig. 1, finally, shows $\langle m_{\beta\beta}\rangle$ as a function of the average mass $\langle m_\beta\rangle = [\Sigma|U_{ei}|^2 m_i^2]^{1/2}$ determined through the analysis of low energy beta decays. The rather large intrinsic width of the $\beta\beta$-decay constraint essentially does not allow one to positively identify the inverted hierarchy, and thus the sign of Δ^2_{atm}, even in combination with these other observables.

It should be noted that systematic uncertainties of the nuclear matrix elements are not folded into the mass limits reported by $\beta\beta$-decay experiments. Taking this additional uncertainty into account would further widen the projections. The uncertainties in oscillation parameterers affect the width of the allowed bands in an asymmetric manner, as shown in Fig. 1. For example, for the degenerate mass pattern ($\langle m_{\beta\beta}\rangle \geq$ 0.1 eV) the upper edge is simply $\langle m_{\beta\beta}\rangle \sim m$, where m is the common mass of the degenerate multiplet, independent of the oscillation parameters, while the lower edge is $m\cos(2\theta_\odot)$. Similar arguments explain the other features of Fig. 1.

If the neutrinoless double beta decay is observed, it will be possible to fix a *range* of absolute values of the masses m_i. Unlike the direct neutrino mass measurements, however, a limit on $\langle m_{\beta\beta}\rangle$ does not allow one to constrain the individual mass values m_i even when the mass differences Δm^2 are known.

Neutrino oscillation data imply, for the first time, the existence of a *lower limit* for the Majorana neutrino mass for some of the mass patterns. Several new double-beta searches have been proposed to probe the interesting $\langle m_{\beta\beta}\rangle$ mass range.

If lepton-number violating right-handed current weak interactions exist, its strength can be characterized by the phenomenological coupling constants η and λ. The $0\nu\beta\beta$ decay rate then depends on $\langle\eta\rangle = \eta\sum_i U_{ei}V_{ei}$ and $\langle\lambda\rangle = \lambda\sum_i U_{ei}V_{ei}$

that vanish for massless or unmixed neutrinos ($V_{\ell j}$ is a matrix analogous to $U_{\ell j}$ but describing the mixing with the hypothetical right-handed neutrinos). This mechanism of the $0\nu\beta\beta$ decay could be, in principle, distinguished from the light Majorana neutrino exchange by the observation of the single electron spectra. The limits on $\langle\eta\rangle$ and $\langle\lambda\rangle$ are listed in a separate table. The reader is cautioned that a number of earlier experiments did not distinguish between η and λ. In addition, see the section on Majoron searches for additional limits set by these experiments.

References

1. V.A. Rodin *et al.*, Phys. Rev. **C68**, 044302 (2003).
2. G.L. Fogli *et al.*, hep-ph/0506083.

Half-life Measurements and Limits for Double-β Decay

In all cases of double-beta decay, (Z,A) $\rightarrow$ (Z+2,A) + $2e^-$ + (0 or 2)$\overline{\nu}_e$. In the following Listings, only best or comparable limits or lifetimes for each isotope are reported. For 2ν decay, which is well established, only measured half-lives are reported.

$t_{1/2}(10^{21}$ yr)	CL%	ISOTOPE	TRANSITION	METHOD	DOCUMENT ID	
• • • We do not use the following data for averages, fits, limits, etc. • • •						
> 1800	90	^{130}Te	0ν	Cryog. det.	[1] ARNABOLDI	05
> 460	90	^{100}Mo	0ν	NEMO-3	[2] ARNOLD	05A
> 100	90	^{82}Se	0ν	NEMO-3	[3] ARNOLD	05A
$(7.11 \pm 0.02 \pm 0.54)$E-3		^{100}Mo	2ν	NEMO-3	[4] ARNOLD	05A
$(9.6 \pm 0.3 \pm 1.0)$E-2		^{82}Se	2ν	NEMO-3	[5] ARNOLD	05A
> 550	90	^{130}Te	0ν	Cryog. det.	[6] ARNABOLDI	04
> 310	90	^{100}Mo	0ν	NEMO-3	[7] ARNOLD	04
> 140	90	^{82}Se	0ν	NEMO-3	[8] ARNOLD	04
$(7.68 \pm 0.02 \pm 0.54)$E-3		^{100}Mo	2ν	NEMO-3	[9] ARNOLD	04
$(10.3 \pm 0.3 \pm 0.7)$E-2		^{82}Se	2ν	NEMO-3	[10] ARNOLD	04
$0.14^{+0.04}_{-0.02} \pm 0.03$	68	^{150}Nd	$0\nu+2\nu$ $0^+ \rightarrow 0^+_1$	γ in Ge det.	[11] BARABASH	04
11900^{+29900}_{-5000}	99.7	^{76}Ge	0ν	Enriched HPGe	[12] KLAPDOR-K...	04A
> 14	90	^{48}Ca	0ν	CaF_2 scint.	[13] OGAWA	04
> 210	90	^{130}Te	0ν	Cryog. det.	[14] ARNABOLDI	03
> 31	90	^{130}Te	0ν $0^+ \rightarrow 2^+$	Cryog. det.	[15] ARNABOLDI	03
$0.61 \pm 0.14^{+0.29}_{-0.35}$	90	^{130}Te	2ν	Cryog. det.	[16] ARNABOLDI	03
> 110	90	^{128}Te	0ν	Cryog. det.	[17] ARNABOLDI	03
$(0.029^{+0.004}_{-0.003})$		^{116}Cd	2ν	$^{116}CdWO_4$ scint.	[18] DANEVICH	03
> 170	90	^{116}Cd	0ν	$^{116}CdWO_4$ scint.	[19] DANEVICH	03

$>$ 29	90	^{116}Cd	0ν	$0^+ \to 2^+$	$^{116}CdWO_4$ scint.	[20]	DANEVICH	03
$>$ 14	90	^{116}Cd	0ν	$0^+ \to 0^+_1$	$^{116}CdWO_4$ scint.	[21]	DANEVICH	03
$>$ 6	90	^{116}Cd	0ν	$0^+ \to 0^+_2$	$^{116}CdWO_4$ scint.	[22]	DANEVICH	03
$1.74 \pm 0.01^{+0.18}_{-0.16}$		^{76}Ge	2ν		Enriched HPGe	[23]	DOERR	03
>15700	90	^{76}Ge	0ν		Enriched HPGe	[24]	AALSETH	02B
$>$ 58	90	^{134}Xe	0ν		Liquid Xe Scint.	[25]	BERNABEI	02D
$>$ 1200	90	^{136}Xe	0ν		Liquid Xe Scint.	[26]	BERNABEI	02D
$15000\ ^{+168000}_{-\ 7500}$		^{76}Ge	0ν		Enriched HPGe	[27]	KLAPDOR-K...	02D
$(7.2 \pm 0.9 \pm 1.8)$E-3		^{100}Mo	2ν		Liq. Ar ioniz.	[28]	ASHITKOV	01
$>$ 4.9	90	^{100}Mo	0ν		Liq. Ar ioniz.	[29]	ASHITKOV	01
$>$ 1.3	90	^{160}Gd	0ν		Gd_2SiO_5:Ce	[30]	DANEVICH	01
$>$ 1.3	90	^{160}Gd	0ν	$0^+ \to 2^+$	Gd_2SiO_5:Ce	[31]	DANEVICH	01
$0.59^{+0.17}_{-0.11} \pm 0.06$		^{100}Mo	$0\nu+2\nu$	$0^+ \to 0^+_1$	Ge coinc.	[32]	DEBRAECKEL...	01
$>$ 55	90	^{100}Mo	$0\nu,\langle m_\nu \rangle$		ELEGANT V	[33]	EJIRI	01
$>$ 42	90	^{100}Mo	$0\nu,\langle \lambda \rangle$		ELEGANT V	[33]	EJIRI	01
$>$ 49	90	^{100}Mo	$0\nu,\langle \eta \rangle$		ELEGANT V	[33]	EJIRI	01
>19000	90	^{76}Ge	0ν		Enriched HPGe	[34]	KLAPDOR-K...	01
$1.55 \pm 0.001^{+0.19}_{-0.15}$	90	^{76}Ge	2ν		Enriched HPGe	[35]	KLAPDOR-K...	01
(9.4 ± 3.2)E-3	90	^{96}Zr	$0\nu+2\nu$		Geochem	[36]	WIESER	01
$0.042^{+0.033}_{-0.013}$		^{48}Ca	2ν		Ge spectrometer	[37]	BRUDANIN	00
$0.021^{+0.008}_{-0.004} \pm 0.002$		^{96}Zr	2ν		NEMO-2	[38]	ARNOLD	99
>1.0	90	^{96}Zr	0ν		NEMO-2	[38]	ARNOLD	99
$(8.3 \pm 1.0 \pm 0.7)$E-2		^{82}Se	2ν		NEMO-2	[39]	ARNOLD	98
$>$ 9.5	90	^{82}Se	0ν		NEMO-2	[40]	ARNOLD	98
$>$ 2.8	90	^{82}Se	0ν	$0^+ \to 2^+$	NEMO-2	[41]	ARNOLD	98
$(7.6^{+2.2}_{-1.4})$E-3		^{100}Mo	2ν		Si(Li)	[42]	ALSTON-...	97
$(6.82^{+0.38}_{-0.53} \pm 0.68)$E-3		^{100}Mo	2ν		TPC	[43]	DESILVA	97
$(6.75^{+0.37}_{-0.42} \pm 0.68)$E-3		^{150}Nd	2ν		TPC	[44]	DESILVA	97
$>$ 1.2	90	^{150}Nd	0ν		TPC	[45]	DESILVA	97
$(3.75 \pm 0.35 \pm 0.21)$E-2		^{116}Cd	2ν	$0^+ \to 0^+$	NEMO 2	[46]	ARNOLD	96
$0.043^{+0.024}_{-0.011} \pm 0.014$		^{48}Ca	2ν		TPC	[47]	BALYSH	96
0.79 ± 0.10		^{130}Te	$0\nu+2\nu$		Geochem	[48]	TAKAOKA	96
$0.61^{+0.18}_{-0.11}$		^{100}Mo	$0\nu+2\nu$	$0^+ \to 0^+_1$	γ in HPGe	[49]	BARABASH	95
$(9.5 \pm 0.4 \pm 0.9)$E-3		^{100}Mo	2ν		NEMO 2		DASSIE	95
$>$ 0.6	90	^{100}Mo	0ν	$0^+ \to 0^+_1$	NEMO 2		DASSIE	95
$0.026^{+0.009}_{-0.005}$		^{116}Cd	2ν	$0^+ \to 0^+$	ELEGANT IV		EJIRI	95
$0.017^{+0.010}_{-0.005} \pm 0.0035$		^{150}Nd	2ν	$0^+ \to 0^+$	TPC		ARTEMEV	93
0.039 ± 0.009		^{96}Zr	$0\nu+2\nu$		Geochem		KAWASHIMA	93
2.7 ± 0.1		^{130}Te	$0\nu+2\nu$		Geochem		BERNATOW...	92
7200 ± 400		^{128}Te	$0\nu+2\nu$		Geochem	[50]	BERNATOW...	92
$>$ 27	68	^{82}Se	0ν	$0^+ \to 0^+$	TPC		ELLIOTT	92
$0.108^{+0.026}_{-0.006}$		^{82}Se	2ν	$0^+ \to 0^+$	TPC		ELLIOTT	92
2.0 ± 0.6		^{238}U	$0\nu+2\nu$		Radiochem	[51]	TURKEVICH	91
$>$ 9.5	76	^{48}Ca	0ν		CaF_2 scint.		YOU	91

$0.12 \pm 0.01 \pm 0.04$	68	^{82}Se	$0\nu+2\nu$	Geochem.	[52] LIN	88
$0.75 \pm 0.03 \pm 0.23$	68	^{130}Te	$0\nu+2\nu$	Geochem.	[53] LIN	88
1800 ± 700	68	^{128}Te	$0\nu+2\nu$	Geochem.	[54] LIN	88B
2.60 ± 0.28		^{130}Te	$0\nu+2\nu$	Geochem	[55] KIRSTEN	83

[1] Supersedes ARNABOLDI 04. Bolometric TeO_2 detector array CUORICINO is used for high resolution search for $0\nu\beta\beta$ decay. The half-life limit is derived from 3.09 kg yr ^{130}Te exposure.

[2] NEMO-3 tracking calorimeter containing 6.9 kg of enriched ^{100}Mo is used in ARNOLD 05A. A limit for $0\nu\beta\beta$ half-life of ^{100}Mo is reported. Supersedes ARNOLD 04.

[3] NEMO-3 tracking calorimeter is used in ARNOLD 05A to place limit on $0\nu\beta\beta$ half-life of ^{82}Se. Detector contains 0.93 kg of enriched ^{82}Se. Supersedes ARNOLD 04.

[4] ARNOLD 05A use the NEMO-3 tracking calorimeter to determine the $2\nu\beta\beta$ half-life of ^{100}Mo with high statistics and low background (389 days of data taking). Supersedes ARNOLD 04.

[5] ARNOLD 05A use the NEMO-3 tracking detector to determine the $2\nu\beta\beta$ half-life of ^{82}Se with high statistics and low background (389 days of data taking). Supersedes ARNOLD 04.

[6] Supersedes ARNABOLDI 03. Bolometric TeO_2 detector array Cuoricino used for high resolution search for $0\nu\beta\beta$ decay.

[7] ARNOLD 04 use the NEMO-3 tracking detector to determine the limit for $0\nu\beta\beta$ halflife of ^{100}Mo. This represents an improvement, by a factor of ~ 6, when compared with EJIRI 01.

[8] ARNOLD 04 use the NEMO-3 tracking detector to determine the limit for $0\nu\beta\beta$ halflife of ^{82}Se. This represents an improvement, by a factor of ~ 10, when compared with ELLIOTT 92. It supersedes the limit of ARNOLD 98 for this decay using NEMO-2.

[9] ARNOLD 04 use the NEMO-3 tracking detector to determine the $2\nu\beta\beta$ halflife of ^{100}Mo with high statistics and low background. The halflife is determined assuming the Single State Dominance. It is in agreement with, and more accurate than, previous determinations. Supersedes DASSIE 95 determination of this quantity with NEMO-2.

[10] ARNOLD 04 use the NEMO-3 tracking detector to determine the $2\nu\beta\beta$ halflife of ^{82}Se. The halflife is in agreement with ARNOLD 98 with NEMO-2 which it supersedes.

[11] BARABASH 04 perform an inclusive measurement of the $\beta\beta$ decay of ^{150}Nd into the first excited (0_1^+) state of ^{150}Sm. Gamma radiation emitted in decay of the excited state is detected.

[12] Supersedes KLAPDOR-KLEINGROTHAUS 02D. Authors present new analysis of event excess seen in Heidelberg-Moscow experiment at $\beta\beta$-decay energy. Enhanced statistics leads to a 4.2 σ evidence for observation of $0\nu\beta\beta$-decay and a finite Majorana neutrino mass. Stated error is purely statistical. No systematic errors are mentioned in the paper. More details can be found in KLAPDOR-KLEINGROTHAUS 04C.

[13] CaF_2 scintillation calorimeter ELEGANT VI used to set limit on $0\nu\beta\beta$-decay rate of ^{48}Ca. The stated half-life limit benefits from a downward fluctuation on the number of background events. The experimental sensitivity is 5.9×10^{21} yr. at 90 % CL. Replaces YOU 91 as the most stringest experiment using ^{48}Ca.

[14] Supersedes ALESSANDRELLO 00. Array of TeO_2 crystals in high resolution cryogenic calorimeter. Some enriched in ^{130}Te. Ground state to ground state decay.

[15] Decay into first excited state of daughter nucleus.

[16] Two neutrino decay into ground state. Relatively large error mainly due to uncertainties in background determination. Reported value is shorter than the geochemical measurements of KIRSTEN 83 and BERNATOWICZ 92 but in agreement with LIN 88 and TAKAOKA 96.

[17] Supersedes ALESSANDRELLO 00. Array of TeO_2 crystals in high resolution cryogenic calorimeter. Some enriched in ^{128}Te. Ground state to ground state decay.

[18] Calorimetric measurement of 2ν ground state decay of ^{116}Cd using enriched $CdWO_4$ scintillators. Agrees with EJIRI 95 and ARNOLD 96. Supersedes DANEVICH 00.

[19] Limit on 0ν decay of ^{116}Cd using enriched $CdWO_4$ scintillators. Supersedes DANEVICH 00.

[20] Limit on 0ν decay of ^{116}Cd into first excited 2^+ state of daughter nucleus using enriched $CdWO_4$ scintillators. Supersedes DANEVICH 00.

[21] Limit on 0ν decay of ^{116}Cd into first excited 0^+ state of daughter nucleus using enriched $CdWO_4$ scintillators. Supersedes DANEVICH 00.

[22] Limit on 0ν decay of ^{116}Cd into second excited 0^+ state of daughter nucleus using enriched $CdWO_4$ scintillators. Supersedes DANEVICH 00.

[23] Results of the Heidelberg-Moscow experiment (KLAPDOR-KLEINGROTHAUS 01 and GUENTHER 97) are reanalyzed using a new simulation of the complete background spectrum. The $\beta\beta 2\nu$-decay rate is deduced from a 41.57 kg-y exposure. The result is in agreement and supersedes the above referenced halflives with similar statistical and systematic errors.

[24] AALSETH 02B limit is based on 117 mol·yr of data using enriched Ge detectors. Background reduction by means of pulse shape analysis is applied to part of the data set. Reported limit is slightly less restrictive than that in KLAPDOR-KLEINGROTHAUS 01 However, it excludes part of the allowed half-life range reported in KLAPDOR-KLEINGROTHAUS 01B for the same nuclide. The analysis has been criticized in KLAPDOR-KLEINGROTHAUS 04B. The criticism was addressed and disputed in AALSETH 04.

[25] BERNABEI 02D report a limit for the 0ν, $0^+ \rightarrow 0^+$ decay of ^{134}Xe, present in the source at 17%, by considering the maximum number of events for this mode compatible with the fitted smooth background.

[26] BERNABEI 02D report a limit for the 0ν, $0^+ \rightarrow 0^+$ decay of ^{136}Xe, by considering the maximum number of events for this mode compatible with the fitted smooth background. The quoted sensitivity is 450×10^{21} yr. The Feldman and Cousins method is used to obtain the quoted limit.

[27] KLAPDOR-KLEINGROTHAUS 02D is an expanded version of KLAPDOR-KLEINGROTHAUS 01B. The authors re-evaluate the data collected by the Heidelberg-Moscow experiment (KLAPDOR-KLEINGROTHAUS 01) and present a more detailed description of their analysis of an excess of counts at the energy expected for neutrinoless double-beta decay. They interpret this excess, which has a significance of 2.2 to 3.1 σ depending on the data analysis, as evidence for the observation of Lepton Number violation and violation of Baryon minus Lepton Number. The analysis has been criticized by AALSETH 02 and others. The criticisms have been addressed in KLAPDOR-KLEINGROTHAUS 02. See also KLAPDOR-KLEINGROTHAUS 02B.

[28] ASHITKOV 01 result for 2ν of ^{100}Mo is in agreement with other determinations of that halflife.

[29] ASHITKOV 01 result for 0ν of ^{100}Mo is less stringent than EJIRI 01.

[30] DANEVICH 01 place limit on 0ν decay of ^{160}Gd using Gd_2SiO_5:Ce crystal scintillators. The limit is more stringent than KOBAYASHI 95.

[31] DANEVICH 01 place limits on 0ν decay of ^{160}Gd into excited 2^+ state of daughter nucleus using Gd_2SiO_5:Ce crystal scintillators.

[32] DEBRAECKELEER 01 performed an inclusive measurement of the $\beta\beta$ decay into the second excited state of the daughter nucleus. A novel coincidence technique counting the de-excitation photons is employed. The result agrees with BARABASH 95.

[33] EJIRI 01 uses tracking calorimeter and isotopically enriched passive source. Efficiencies were calculated assuming $\langle m_\nu \rangle$, $\langle \lambda \rangle$, or $\langle \eta \rangle$ driven decay. This is a continuation of EJIRI 96 which it supersedes.

[34] KLAPDOR-KLEINGROTHAUS 01 is a continuation of the work published in BAUDIS 99. Isotopically enriched Ge detectors are used in calorimetric measurement. The most stringent bound is derived from the data set in which pulse-shape analysis has been used to reduce background. Exposure time is 35.5 kg y. Supersedes BAUDIS 99 as most stringent result.

[35] KLAPDOR-KLEINGROTHAUS 01 is a measurement of the $\beta\beta 2\nu$-decay rate with higher statistics than GUENTHER 97. The reported value has a larger systematic error than their previous result.

[36] WIESER 01 reports an inclusive geochemical measurement of ^{96}Zr $\beta\beta$ half life. Their result agrees within 2σ with ARNOLD 99 but only marginally, within 3σ, with KAWASHIMA 93.

[37] BRUDANIN 00 determine the 2ν halflife of ^{48}Ca. Their value is less accurate than BALYSH 96.

[38] ARNOLD 99 measure directly the 2ν decay of Zr for the first time, using the NEMO-2 tracking detector and an isotopically enriched source. The lifetime is more accurate than the geochemical result of KAWASHIMA 93.

[39] ARNOLD 98 measure the 2ν decay of ^{82}Se by comparing the spectra in an enriched and natural selenium source using the NEMO-2 tracking detector. The measured half-life is in agreement, perhaps slightly shorter, than ELLIOTT 92.

[40] ARNOLD 98 determine the limit for 0ν decay to the ground state of ^{82}Se using the NEMO-2 tracking detector. The half-life limit is in agreement, but less stringent, than ELLIOTT 92.

[41] ARNOLD 98 determine the limit for 0ν decay to the excited 2^+ state of ^{82}Se using the NEMO-2 tracking detector.

[42] ALSTON-GARNJOST 97 report evidence for 2ν decay of ^{100}Mo. This decay has been also observed by EJIRI 91, DASSIE 95, and DESILVA 97.

[43] DESILVA 97 result for 2ν decay of ^{100}Mo is in agreement with ALSTON-GARNJOST 97 and DASSIE 95. This measurement has the smallest errors.

[44] DESILVA 97 result for 2ν decay of ^{150}Nd is in marginal agreement with ARTEMEV 93. It has smaller errors.

[45] DESILVA 97 do not explain whether their efficiency for 0ν decay of ^{150}Nd was calculated under the assumption of a $\langle m_\nu \rangle$, $\langle \lambda \rangle$, or $\langle \eta \rangle$ driven decay.

[46] ARNOLD 96 measure the 2ν decay of ^{116}Cd. This result is in agreement with EJIRI 95, but has smaller errors. Supersedes ARNOLD 95.

[47] BALYSH 96 measure the 2ν decay of ^{48}Ca, using a passive source of enriched ^{48}Ca in a TPC.

[48] TAKAOKA 96 measure the geochemical half-life of ^{130}Te. Their value is in disagreement with the quoted values of BERNATOWICZ 92 and KIRSTEN 83; but agrees with several other unquoted determinations, e.g., MANUEL 91.

[49] BARABASH 95 cannot distinguish 0ν and 2ν, but it is inferred indirectly that the 0ν mode accounts for less than 0.026% of their event sample. They also note that their result disagrees with the previous experiment by the NEMO group (BLUM 92).

[50] BERNATOWICZ 92 finds ^{128}Te/^{130}Te activity ratio from slope of ^{128}Xe/^{132}Xe vs ^{130}Xe/^{132}Xe ratios during extraction, and normalizes to lead-dated ages for the ^{130}Te lifetime. The authors state that their results imply that "(a) the double beta decay of ^{128}Te has been firmly established and its half-life has been determined ... without any ambiguity due to trapped Xe interferences... (b) Theoretical calculations ... underestimate the [long half-lives of ^{128}Te ^{130}Te] by 1 or 2 orders of magnitude, pointing to a real suppression in the 2ν decay rate of these isotopes. (c) Despite [this], most $\beta\beta$-models predict a *ratio* of 2ν decay widths ... in fair agreement with observation." Further details of the experiment are given in BERNATOWICZ 93. Our listed half-life has been revised downward from the published value by the authors, on the basis of reevaluated cosmic-ray ^{128}Xe production corrections.

[51] TURKEVICH 91 observes activity in old U sample. The authors compare their results with theoretical calculations. They state "Using the phase-space factors of Boehm and Vogel (BOEHM 87) leads to matrix element values for the ^{238}U transition in the same range as deduced for ^{130}Te and ^{76}Ge. On the other hand, the latest theoretical estimates (STAUDT 90) give an upper limit that is 10 times lower. This large discrepancy implies either a defect in the calculations or the presence of a faster path than the standard two-neutrino mode in this case." See BOEHM 87 and STAUDT 90.

[52] Result agrees with direct determination of ELLIOTT 92.

[53] Inclusive half life inferred from mass spectroscopic determination of abundance of $\beta\beta$-decay product ^{130}Te in mineral kitkaite (NiTeSe). Systematic uncertainty reflects variations in U-Xe gas-retention-age derived from different uranite samples. Agrees with geochemical determination of TAKAOKA 96 and direct measurement of ARNABOLDI 03. Inconsistent with results of KIRSTEN 83 and BERNATOWICZ 92.

[54] Ratio of inclusive double beta half lives of ^{128}Te and ^{130}Te determined from minerals melonite ($NiTe_2$) and altaite (PbTe) by means of mass spectroscopic measurement of abundance of $\beta\beta$-decay products. As gas-retention-age could not be determined the authors use half life of ^{130}Te (LIN 88) to infer the half life of ^{128}Te. No estimate of the systematic uncertainty of this method is given. The directly determined half life ratio agrees with BERNATOWICZ 92. However, the inferred ^{128}Te half life disagrees with KIRSTEN 83 and BERNATOWICZ 92.

[55] KIRSTEN 83 reports "2σ" error. References are given to earlier determinations of the ^{130}Te lifetime.

$\langle m_\nu \rangle$, The Effective Weighted Sum of Majorana Neutrino Masses Contributing to Neutrinoless Double-β Decay

$\langle m_\nu \rangle = |\Sigma\ U_{1j}^2 m_{\nu_j}|$, where the sum goes from 1 to n and where n = number of neutrino generations, and ν_j is a Majorana neutrino. Note that U_{ej}^2, not $|U_{ej}|^2$, occurs in the sum. The possibility of cancellations has been stressed. In the following Listings, only best or comparable limits or lifetimes for each isotope are reported.

VALUE (eV)	*CL%*	*ISOTOPE*	*TRANSITION*	*METHOD*	*DOCUMENT ID*	
• • • We do not use the following data for averages, fits, limits, etc. • • •						
< 0.2–1.1	90	^{130}Te		Cryog. det.	[56] ARNABOLDI	05
< 0.7–2.8	90	^{100}Mo	0ν	NEMO-3	[57] ARNOLD	05A
< 1.7–4.9	90	^{82}Se	0ν	NEMO-3	[58] ARNOLD	05A
< 0.37–1.9	90	^{130}Te		Cryog. det.	[59] ARNABOLDI	04
< 0.8–1.2	90	^{100}Mo	0ν	NEMO-3	[60] ARNOLD	04
< 1.5–3.1	90	^{82}Se	0ν	NEMO-3	[60] ARNOLD	04
0.1–0.9	99.7	^{76}Ge		Enriched HP Ge	[61] KLAPDOR-K...	04A
< 7.2–44.7	90	^{48}Ca		CaF_2 scint.	[62] OGAWA	04
$<$ 1.1–2.6	90	^{130}Te		Cryog. det.	[63] ARNABOLDI	03
< 1.5–1.7	90	^{116}Cd	0ν	$^{116}CdWO_4$ scint.	[64] DANEVICH	03
< 0.33–1.35	90			Enriched HPGe	[65] AALSETH	02B
<2.9	90	^{136}Xe	0ν	Liquid Xe Scint.	[66] BERNABEI	02D
$0.39^{+0.17}_{-0.28}$		^{76}Ge	0ν	Enriched HPGe	[67] KLAPDOR-K...	02D
< 2.1–4.8	90	^{100}Mo	0ν	ELEGANT V	[68] EJIRI	01
< 0.35	90	^{76}Ge		Enriched HPGe	[69] KLAPDOR-K...	01
<23	90	^{96}Zr		NEMO-2	[70] ARNOLD	99
< 1.1–1.5		^{128}Te		Geochem	[71] BERNATOW...	92
<5	68	^{82}Se		TPC	[72] ELLIOTT	92
<8.3	76	^{48}Ca	0ν	CaF_2 scint.	YOU	91

[56] Supersedes ARNABOLDI 04. Reported range of limits due to use of different nuclear matrix element calculations.

[57] Mass limits reported in ARNOLD 05A are derived from ^{100}Mo data, obtained by the NEMO-3 collaboration. The range reflects the spread of matrix element calculations considered in this work. Supersedes ARNOLD 04.

[58] Neutrino mass limits based on ^{82}Se data utilizing the NEMO-3 detector. The range reported in ARNOLD 05A reflects the spread of matrix element calculations considered in this work. Supersedes ARNOLD 04.

[59] Supersedes ARNABOLDI 03. Reported range of limits due to use of different nuclear matrix element calculations.
[60] ARNOLD 04 limit is based on the nuclear matrix elements of SIMKOVIC 99, STOICA 01 and CIVITARESE 03.
[61] Supersedes KLAPDOR-KLEINGROTHAUS 02D. Event excess at $\beta\beta$-decay energy is used to derive Majorana neutrino mass using the nuclear matrix elements of STAUDT 90. The mass range shown is based on the authors evaluation of the uncertainties of the STAUDT 90 matrix element calculation. If this uncertainty is neglected, and only statistical errors are considered, the range in $\langle m \rangle$ becomes (0.2–0.6) eV at the 3 σ level.
[62] Calorimetric CaF_2 scintillator. Range of limits reflects authors' estimate of the uncertainty of the nuclear matrix elements. Replaces YOU 91 as the most stringest limit based on ^{48}Ca.
[63] Supersedes ALESSANDRELLO 00. Cryogenic calorimeter search. Reported a range reflecting uncertainty in nuclear matrix element calculations.
[64] Limit for $\langle m_\nu \rangle$ is based on the nuclear matrix elements of STAUDT 90 and ARNOLD 96. Supersedes DANEVICH 00.
[65] AALSETH 02B reported range of limits on $\langle m_\nu \rangle$ reflects the spread of theoretical nuclear matrix elements. Excludes part of allowed mass range reported in KLAPDOR-KLEINGROTHAUS 01B.
[66] BERNABEI 02D limit is based on the matrix elements of SIMKOVIC 02. The range of neutrino masses based on a variety of matrix elements is 1.1–2.9 eV.
[67] KLAPDOR-KLEINGROTHAUS 02D is a detailed description of the analysis of the data collected by the Heidelberg-Moscow experiment, previously presented in KLAPDOR-KLEINGROTHAUS 01B. Matrix elements in STAUDT 90 have been used. See the footnote in the preceding table for further details. See also KLAPDOR-KLEINGROTHAUS 02B.
[68] The range of the reported $\langle m_\nu \rangle$ values reflects the spread of the nuclear matrix elements. On axis value assuming $\langle\lambda\rangle$=$\langle\eta\rangle$=0.
[69] KLAPDOR-KLEINGROTHAUS 01 uses the calculation by STAUDT 90. Using several other models in the literature could worsen the limit up to 1.2 eV. This is the most stringent experimental bound on m_ν. It supersedes BAUDIS 99B.
[70] ARNOLD 99 limit based on the nuclear matrix elements of STAUDT 90.
[71] BERNATOWICZ 92 finds these majorana neutrino mass limits assuming that the measured geochemical decay width is a limit on the 0ν decay width. The range is the range found using matrix elements from HAXTON 84, TOMODA 87, and SUHONEN 91. Further details of the experiment are given in BERNATOWICZ 93.
[72] ELLIOTT 92 uses the matrix elements of HAXTON 84.

Limits on Lepton-Number Violating ($V+A$) Current Admixture

For reasons given in the discussion at the beginning of this section, we list only results from 1989 and later. $\langle\lambda\rangle = \lambda\sum U_{ej}V_{ej}$ and $\langle\eta\rangle = \eta\sum U_{ej}V_{ej}$, where the sum is over the number of neutrino generations. This sum vanishes for massless or unmixed neutrinos. In the following Listings, only best or comparable limits or lifetimes for each isotope are reported.

$\langle\lambda\rangle$ (10^{-6})	CL%	$\langle\eta\rangle$ (10^{-8})	CL%	ISOTOPE	METHOD	DOCUMENT ID	
• • • We do not use the following data for averages, fits, limits, etc. • • •							
<2.5	90			^{100}Mo	0ν, NEMO-3	[73] ARNOLD	05A
<3.8	90			^{82}Se	0ν, NEMO-3	[74] ARNOLD	05A
< 1.5–2.0	90			^{100}Mo	0ν, NEMO-3	[75] ARNOLD	04
< 3.2–3.8	90			^{82}Se	0ν, NEMO-3	[76] ARNOLD	04
< 1.6–2.4	90	< 0.9–5.3	90	^{130}Te	Cryog. det.	[77] ARNABOLDI	03

<2.2	90	<2.5	90	^{116}Cd	$^{116}CdWO_4$ scint.	[78] DANEVICH	03
< 3.2–4.7	90	< 2.4–2.7	90	^{100}Mo	ELEGANT V	[79] EJIRI	01
<1.1	90	<0.64	90	^{76}Ge	Enriched HPGe	[80] GUENTHER	97
<4.4	90	<2.3	90	^{136}Xe	TPC	[81] VUILLEUMIER	93
		<5.3		^{128}Te	Geochem	[82] BERNATOW...	92

[73] ARNOLD 05A derive limit for $\langle\lambda\rangle$ based on ^{100}Mo data collected with NEMO-3 detector. No limit for $\langle\eta\rangle$ is given. Supersedes ARNOLD 04.

[74] ARNOLD 05A derive limit for $\langle\lambda\rangle$ based on ^{82}Se data collected with NEMO-3 detector. No limit for $\langle\eta\rangle$ is given. Supersedes ARNOLD 04.

[75] ARNOLD 04 use the matrix elements of SUHONEN 94 to obtain a limit for $\langle\lambda\rangle$, no limit for $\langle\eta\rangle$ is given. This limit is more stringent than the limit in EJIRI 01 for the same nucleus.

[76] ARNOLD 04 use the matrix elements of TOMODA 91 and SUHONEN 91 to obtain a limit for $\langle\lambda\rangle$, no limit for $\langle\eta\rangle$ is given.

[77] Supersedes ALESSANDRELLO 00. Cryogenic calorimeter search. Reported a range reflecting uncertainty in nuclear matrix element calculations.

[78] Limits for $\langle\lambda\rangle$ and $\langle\eta\rangle$ are based on nuclear matrix elements of STAUDT 90. Supersedes DANEVICH 00.

[79] The range of the reported $\langle\lambda\rangle$ and $\langle\eta\rangle$ values reflects the spread of the nuclear matrix elements. On axis value assuming $\langle m_\nu\rangle$=0 and $\langle\lambda\rangle$=$\langle\eta\rangle$=0, respectively.

[80] GUENTHER 97 limits use the matrix elements of STAUDT 90. Supersedes BALYSH 95 and BALYSH 92.

[81] VUILLEUMIER 93 uses the matrix elements of MUTO 89. Based on a half-life limit 2.6×10^{23} y at 90%CL.

[82] BERNATOWICZ 92 takes the measured geochemical decay width as a limit on the 0ν width, and uses the SUHONEN 91 coefficients to obtain the least restrictive limit on η. Further details of the experiment are given in BERNATOWICZ 93.

Double-β Decay REFERENCES

ARNABOLDI	05	PRL 95 142501	C. Arnaboldi *et al.*	(CUORICINO Collab.)
ARNOLD	05A	PRL 95 182302	R. Arnold *et al.*	(NEMO-3 Collab.)
AALSETH	04	PR D70 078302	C.E. Aalseth *et al.*	
ARNABOLDI	04	PL B584 260	C. Arnaboldi *et al.*	
ARNOLD	04	JETPL 80 377	R. Arnold *et al.*	(NEMO3 Detector Collab.)
		Translated from ZETFP 80 429.		
BARABASH	04	JETPL 79 10	A.S. Barabash *et al.*	
KLAPDOR-K...	04A	PL B586 198	H.V. Klapdor-Kleingrothaus *et al.*	
KLAPDOR-K...	04B	PR D70 078301	H.V. Klapdor-Kleingrothaus, A. Dietz, I.V. Krivosheina	
KLAPDOR-K...	04C	NIM A522 371	H.V. Klapdor-Kleingrothaus *et al.*	
OGAWA	04	NP A730 215	I. Ogawa *et al.*	
ARNABOLDI	03	PL B557 167	C. Arnaboldi *et al.*	
CIVITARESE	03	NP A729 867	O. Civitarese, J. Suhonen	
DANEVICH	03	PR C68 035501	F.A. Danevich *et al.*	
DOERR	03	NIM A513 596	C. Doerr, H.V. Klapdor-Kleingrothaus	
AALSETH	02	MPL A17 1475	C.E. Aalseth *et al.*	
AALSETH	02B	PR D65 092007	C.E. Aalseth *et al.*	(IGEX Collab.)
BERNABEI	02D	PL B546 23	R. Bernabei *et al.*	(DAMA Collab.)
KLAPDOR-K...	02	hep-ph/0205228	H.V. Klapdor-Kleingrothaus	
KLAPDOR-K...	02B	JINRRC 110 57	H.V. Klapdor-Kleingrothaus, A. Dietz, I.V. Krivosheina	
KLAPDOR-K...	02D	FP 32 1181	H.V. Klapdor-Kleingrothaus, A. Dietz, I.V. Krivosheina	
SIMKOVIC	02	hep-ph/0204278	F. Simkovic, P. Domin, A. Faessler	
ASHITKOV	01	JETPL 74 529	V.D. Ashitkov *et al.*	
		Translated from ZETFP 74 601.		
DANEVICH	01	NP A694 375	F.A. Danevich *et al.*	
DEBRAECKEL...	01	PRL 86 3510	L. De Braeckeleer *et al.*	
EJIRI	01	PR C63 065501	H. Ejiri *et al.*	
KLAPDOR-K...	01	EPJ A12 147	H.V. Klapdor-Kleingrothaus *et al.*	
KLAPDOR-K...	01B	MPL A16 2409	H.V. Klapdor-Kleingrothaus *et al.*	
STOICA	01	NP A694 269	S. Stoica, H.V. Klapdor-Kleingrothous	

WIESER	01	PR C64 024308	M.E. Wieser, J.R. De Laeter	
ALESSAND...	00	PL B486 13	A. Alessandrello *et al.*	
BRUDANIN	00	PL B495 63	V.B. Brudanin *et al.*	
DANEVICH	00	PR C62 045501	F.A. Danevich *et al.*	
ARNOLD	99	NP A658 299	R. Arnold *et al.*	(NEMO Collab.)
BAUDIS	99	PR D59 022001	L. Baudis *et al.*	(Heidelberg-Moscow Collab.)
BAUDIS	99B	PRL 83 41	L. Baudis *et al.*	(Heidelberg-Moscow Collab.)
SIMKOVIC	99	PR C60 055502	F. Simkovic *et al.*	
ARNOLD	98	NP A636 209	R. Arnold *et al.*	(NEMO-2 Collab.)
ALSTON-...	97	PR C55 474	M. Alston-Garnjost *et al.*	(LBL, MTHO+)
DESILVA	97	PR C56 2451	A. de Silva *et al.*	(UCI)
GUENTHER	97	PR D55 54	M. Gunther *et al.*	(Heidelberg-Moscow Collab.)
ARNOLD	96	ZPHY C72 239	R. Arnold *et al.*	(BCEN, CAEN, JINR+)
BALYSH	96	PRL 77 5186	A. Balysh *et al.*	(KIAE, UCI, CIT)
EJIRI	96	NP A611 85	H. Ejiri *et al.*	(OSAK)
TAKAOKA	96	PR C53 1557	N. Takaoka, Y. Motomura, K. Nagao	(KYUSH, OKAY)
ARNOLD	95	JETPL 61 170 Translated from ZETFP 61 168.	R.G. Arnold *et al.*	(NEMO Collab.)
BALYSH	95	PL B356 450	A. Balysh *et al.*	(Heidelberg-Moscow Collab.)
BARABASH	95	PL B345 408	A.S. Barabash *et al.*	(ITEP, SCUC, PNL+)
DASSIE	95	PR D51 2090	D. Dassie *et al.*	(NEMO Collab.)
EJIRI	95	JPSJ 64 339	H. Ejiri *et al.*	(OSAK, KIEV)
KOBAYASHI	95	NP A586 457	M. Kobayashi, M. Kobayashi	(KEK, SAGA)
SUHONEN	94	PR C49 3055	J. Suhonen, O. Civitarese	
ARTEMEV	93	JETPL 58 262 Translated from ZETFP 58 256.	V.A. Artemiev *et al.*	(ITEP, INRM)
BERNATOW...	93	PR C47 806	T. Bernatowicz *et al.*	(WUSL, TATA)
KAWASHIMA	93	PR C47 R2452	A. Kawashima, K. Takahashi, A. Masuda	(TOKYC+)
VUILLEUMIER	93	PR D48 1009	J.C. Vuilleumier *et al.*	(NEUC, CIT, VILL)
BALYSH	92	PL B283 32	A. Balysh *et al.*	(MPIH, KIAE, SASSO)
BERNATOW...	92	PRL 69 2341	T. Bernatowicz *et al.*	(WUSL, TATA)
BLUM	92	PL B275 506	D. Blum *et al.*	(NEMO Collab.)
ELLIOTT	92	PR C46 1535	S.R. Elliott *et al.*	(UCI)
EJIRI	91	PL B258 17	H. Ejiri *et al.*	(OSAK)
MANUEL	91	JPG 17 S221	O.K. Manuel	(MISSR)
SUHONEN	91	NP A535 509	J. Suhonen, S.B. Khadkikar, A. Faessler	(JYV+)
TOMODA	91	RPP 54 53	T. Tomoda	
TURKEVICH	91	PRL 67 3211	A. Turkevich, T.E. Economou, G.A. Cowan	(CHIC+)
YOU	91	PL B265 53	K. You *et al.*	(BHEP, CAST+)
STAUDT	90	EPL 13 31	A. Staudt, K. Muto, H.V. Klapdor-Kleingrothaus	
MUTO	89	ZPHY A334 187	K. Muto, E. Bender, H.V. Klapdor	(TINT, MPIH)
LIN	88	NP A481 477	W.J. Lin *et al.*	
LIN	88B	NP A481 484	W.J. Lin *et al.*	
BOEHM	87	Massive Neutrinos Cambridge Univ. Press, Cambridge	F. Bohm, P. Vogel	(CIT)
TOMODA	87	PL B199 475	T. Tomoda, A. Faessler	(TUBIN)
HAXTON	84	PPNP 12 409	W.C. Haxton, G.J. Stevenson	
KIRSTEN	83	PRL 50 474	T. Kirsten, H. Richter, E. Jessberger	(MPIH)